Warming exacerbates global inequality in forest carbon and nitrogen cycles

Jinglan Cui [1,2], Ouping Deng[1,3], Miao Zheng[1], Xiuming Zhang [1,4], Zihao Bian [5,6], Naiqing Pan[5], Hanqin Tian [5], Jianming Xu[1,7] & Baojing Gu [1,8] ✉

Forests are invaluable natural resources that provide essential services to humanity. However, the effects of global warming on forest carbon and nitrogen cycling remain uncertain. Here we project a decrease in total nitrogen input and accumulation by 7 ± 2 and 28 ± 9 million tonnes (Tg), respectively, and an increase in reactive nitrogen losses to the environment by 9 ± 3 Tg for 2100 due to warming in a fossil-fueled society. This would compromise the global carbon sink capacity by 0.45 ± 0.14 billion tonnes annually. Furthermore, warming-induced inequality in forest carbon and nitrogen cycles could widen the economic gap between the Global South and Global North. High-income countries are estimated to gain US$179 billion in benefits from forest assets under warming, while other regions could face net damages of US$31 billion. Implementing climate-smart forest management, such as comprehensive restoration and optimizing tree species composition, is imperative in the face of future climate change.

Forests harbor over 75% of the Earth's terrestrial biodiversity and serve as natural assets in tropical, temperate, and boreal biomes[1]. Their lush canopies provide humanity with essential ecosystem services and resources, including carbon sequestration, regulation of the hydrological cycle and microclimates, and the provision of forest products[2,3]. Forests support the livelihoods of 1.6 billion people, particularly some impoverished populations residing in mountainous regions of the Global South[4]. Global warming poses potential risks to the structure and functions of forests[5]. The processes governing carbon and nitrogen cycling in forests are sensitive to the rising temperatures[6]. The response of certain variables to temperature changes follows parabolic trajectories, reaching their peak reaction rates at optimal temperatures, such as ecosystem respiration[7] and biological nitrogen fixation (BNF)[8]. Moderate temperature increases have the potential to promote biological reaction rates and extend the plant growing season, thereby increasing overall plant productivity[9]. Conversely, extreme heat can increase plant transpiration rates, enhancing water vapor loss and reducing productivity[10].

Temperature sensitivity also affects soil denitrification processes in forests, as evidenced by mean Q_{10} values of 2.3 ± 0.5[11]. This indicates a likely increase in nitrogen losses into the surrounding environment with rising temperatures. However, the responses of many variables involved in biogeochemical cycling to warming can be divergent and exhibit spatial and temporal heterogeneity[9,12]. Such complex interplays could alter the traditional roles of forests across various landscapes, thereby influencing socio-economic trajectories[13,14]. Despite this, there is a lack of comprehensive research exploring the effects of warming on the holistic nitrogen cycle and the nuanced interactions between carbon and nitrogen within forests, especially at finer resolutions[6,15]. There is an immediate need for accurate economic assessments that describe the impacts of warming-induced changes on forest assets, based on empirical data and state-of-the-art biogeochemical models[16].

[1]College of Environmental and Resource Sciences, Zhejiang University, Hangzhou, China. [2]Policy Simulation Laboratory, Zhejiang University, Hangzhou, China. [3]College of Resources, Sichuan Agricultural University, Chengdu, China. [4]International Institute for Applied Systems Analysis, Laxenburg, Austria. [5]Schiller Institute for Integrated Science and Society, Department of Earth and Environmental Sciences, Boston College, Chestnut Hill, MA, USA. [6]School of Geography, Nanjing Normal University, Nanjing, China. [7]Zhejiang Provincial Key Laboratory of Agricultural Resources and Environment, Zhejiang University, Hangzhou, China. [8]Ministry of Education Key Laboratory of Environment Remediation and Ecological Health, Zhejiang University, Hangzhou, China. ✉e-mail: bjgu@zju.edu.cn

The primary objective of this study is to investigate how climate warming affects the carbon and nitrogen cycling in global forests, providing a scientific basis for refining Earth system models and designing effective forest management policies to address the challenges posed by global warming. To achieve this goal, we first compile a comprehensive global dataset of warming experiments to explore the underlying mechanisms of forest carbon and nitrogen cycle responses to warming. We then employ a multi-model strategy to project the carbon and nitrogen trajectories in global forests from 2040 to 2100 under future warming scenarios. Finally, we assess the impacts of warming on forest assets in terms of ecosystem well-being, climate influence, and forest production using a cost-effective approach.

Results and discussion

Forest carbon and nitrogen cycles responses to warming

A notable shift was observed in the global land surface temperature along latitudinal gradients in the first two decades of the 21st century (2001–2020), averaging a 1.3 °C increase relative to 1961–1980, with distinct variations in specific terrestrial regions (Fig. 1a). The Eurasian landmass, particularly near the 71 °N latitude in the Northern Hemisphere, experienced the most pronounced warming—temperatures increased by up to 3.7 °C. In contrast, the Southern Hemisphere experienced the most significant warming at 26°S latitude, with an increase of up to 1.5 °C. Various warming techniques, including heating cables, infrared radiators, open-top chambers, curtains, and greenhouses, have been used in forest study sites to mimic higher envir-
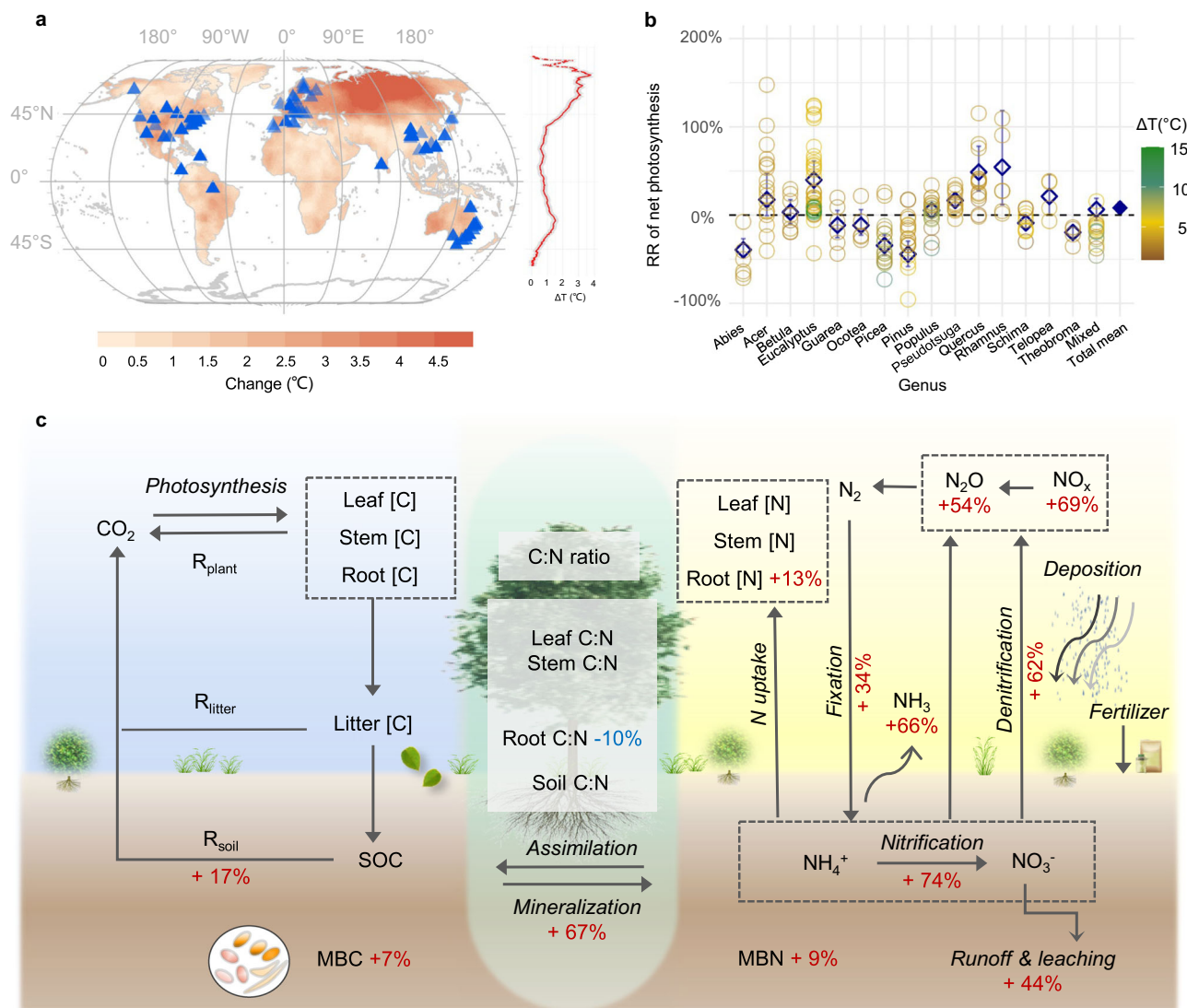

Fig. 1 | Responses of carbon and nitrogen cycles to warming in global forests. **a** Changes in land surface temperature (ΔT) during 2001–2020 relative to 1961-1980 (left panel) and ΔT by latitude (right panel). The blue triangles represent warming experimental sites across global forests. **b** Response ratios (RR) of net photosynthesis to warming categorized by vegetation genus. The diamonds with error bars show the mean values of the RRs with 95% confidence intervals. Scatter plots represent RRs from different observations in warming experiments, with the color gradient indicating the warming magnitude (ΔT, temperature difference between warming treatment and control). The different responses to experimental warming among different genera and species suggest potential mechanisms of competition and succession under warming. The sample size for the overall mean is 285. **c** A schematic representation of the carbon cycle, nitrogen cycle, and carbon-nitrogen interactions in response to warming. Red percentages indicate significant increases in global mean RR, while the blue percentages indicate significant decreases. The global mean manipulation magnitude in warming experiments is 3.8 °C. [C] carbon content, R_x stands for the respiration of component x where x can be plant, litter, and soil, SOC soil organic carbon, MBC microbial biomass carbon, [N] nitrogen content, MBN microbial biomass nitrogen. Source data are provided as a Source Data file.

onmental temperatures[17–20]. Our comprehensive global synthesis of these warming experiments underscores that experimental warming broadly promotes carbon cycling, including both productivity and respiration.

Specifically, warming contributes to an 8% increase in vegetation net primary productivity (NPP) (95% CI: 2% to 15%) (Fig. 1b). This finding aligns with other studies based on warming experiments and Earth system models, primarily attributing this increase to prolonged growing seasons and enhanced photosynthetic activity in warmer climates[9]. Currently, most vegetation, with some exceptions in tropical forests, has not reached its optimal ecosystem-level temperature for photosynthesis under the prevailing climate conditions[21]. Thus, moderate warming generally promotes overall vegetation growth. Meanwhile, warming tends to drive competition and succession within forest ecosystems, as different genera and species respond differently to experimental warming (Fig. 1b). For example, dominant boreal tree species such as *Abies balsamea* and *Pinus banksiana* in Minnesota have shown decreased NPP and higher mortality under experimental warming, whereas certain temperate species such as *Acer rubrum* and *Quercus rubra* have thrived, suggesting that these distinct productivity responses could lead to potential shifts in species dominance, competition, and succession within forests[12]. Notably, even within a single species, different genotypes show different growth responses to warming—as exemplified by the coastal and upland genotypes of an Australian plant *Telopea speciosissima*[22]. Additionally, some genera (e.g., *Acer*, *Eucalyptus*) show higher variability in productivity responses relative to others (Fig. 1b). While we cannot fully explain this variability, we discuss some potential influencing factors in the Supplementary Discussion. These divergences imply that warming will recalibrate competitive balances, favoring species better adapted to warmer climates and accelerating the evolution of forest communities.

Moreover, experimental warming was found to increase soil respiration by 17% (12–21%) (Fig. 1c), due to enhanced carbon dioxide emissions from soil microbes, plant roots, and their mycorrhizal fungi. The suppressed root carbon to nitrogen (C:N) ratio (−10%, −17% to −4%) suggests a likely trend towards increased decomposition of soil organic matter (Fig. 1c), contributing to higher heterotrophic respiration under warming[23]. Concurrently, microbial biomass carbon exhibits a mean positive response of 7% (2% to 12%), indicating a general increase in microbial activity in forests under warming, consistent with a previous meta-analysis[24]. However, microbial biomass carbon can show negative responses to warming in some instances, which might be associated with substrate limitations specific to the field sites, such as phosphorus constraints[25–27].

In parallel, the nitrogen cycle demonstrates accelerated responses to experimental warming. Numerous nitrogen transformation processes, predominantly mediated by microbes[28], tend to accelerate within a certain temperature range due to stimulated microbial activity. This leads to significant increases in processes such as mineralization (+67%, 52% to 84%), BNF (+34%, 3% to 74%), nitrification (+74%, 59% to 95%), and denitrification (+62%, 37% to 91%) (Fig. 1c). Notably, these processes generally intensify with rising temperatures until they reach their respective optimal temperature thresholds, which have been previously identified by empirical data synthesis—for BNF, this threshold is around 25 °C[8], while for denitrification, it can exceed 40 °C, reflecting the diverse denitrifying microbial community[29]. In addition, experimental warming induces changes in ecosystem nitrogen content. Both root nitrogen content and microbial biomass nitrogen increased by 13% (6–25%) and 9% (0.4–20%), respectively. Warming enhanced nitrogen cycling activity in the most microbiologically active root zones in the surface soil, leading to substantial increases in various forms of reactive nitrogen losses (N_r), including gaseous emissions such as ammonia (NH_3, +66%, 23–124%), nitrous oxide (N_2O, +54%, 1–135%), nitrogen oxides (NO_x, mainly nitric oxide and nitrogen dioxide, +69%, 44–99%), and

increased nitrate (NO_3^-, + 44%, 1–122%) leaching and runoff to aquatic systems (Fig. 1c).

Overall, warming accelerates both carbon and nitrogen cycling, increasing productivity but also causing more N_r loss. In our analysis, the C:N ratios for leaf, stem, root, and soil were considered key variables for understanding carbon–nitrogen interactions in response to warming. We found that warming generally does not affect the C:N ratios in forest plants and soil, except for a lower root C:N ratio, which is mainly due to an increase in root nitrogen content (Fig. 1c).

Spatial inequality of nitrogen and carbon cycles under warming

We develop a global-scale forest carbon-nitrogen cycle model by integrating a multi-model strategy based on the Dynamic Land Ecosystem Model (DLEM)[30,31] and Coupled Human and Natural Systems (CHANS) models[32,33] (see Supplementary Methods for details and rationale).

This model aims to project carbon and nitrogen budgets under different scenarios, including baseline and warming scenarios formulated through Shared Socioeconomic Pathways (SSP) and Representative Concentration Pathways (RCP) (Supplementary Fig. 1). Our approach allows us to examine the spatiotemporal dynamics of global carbon and nitrogen budgets from 2040 to 2100 under future warming conditions, in contrast to the baseline metrics. In our baseline scenarios, we establish three sub-scenarios: a sustainable society (SSP1), a middle-of-the-road society (SSP2), and a fossil-fueled society (SSP5). These baseline scenarios are based on a counterfactual assumption that the Earth's temperatures have plateaued since 2020. Conversely, our warming scenarios are divided into three sub-scenarios: a sustainable society with SSP1-2.6, a middle-of-the-road society with SSP2-4.5, and a fossil-fueled society with SSP5-8.5. These are aligned with different levels of radiative forcing from RCP2.6, RCP4.5, to RCP8.5, respectively, encompassing a range from low to high emissions. Our results suggest pronounced spatial variations in the expected evolution of carbon and nitrogen cycles in global forests under the SSP5-8.5 warming scenario for 2100, related to factors such as latitude, altitude, and climate zones (Fig. 2). In particular, negative changes in nitrogen inputs, nitrogen-containing forest products (N products), and carbon sink (C sink, net biome productivity) tend to be more pronounced and widespread at lower latitudes and altitudes than at higher latitudes and altitudes. Moreover, potential increases in N_r loss, decreases in nitrogen accumulation in biomass and soil (N accumulation), and reductions in nitrogen use efficiency (NUE) are likely to be predominant globally.

At the global forest scale, possible trends indicate an 8% decrease in nitrogen inputs, an 18% increase in N products, a 48% increase in N_r losses, and a 75% decrease in N accumulation under the SSP5-8.5 warming scenario for 2100 relative to the baseline scenario (Figs. 2 and 3). Consequently, global NUE is likely to decrease from 66% to 43% due to warming. Despite the potential for increased forest turnover and productivity under future warming, the confluence of reduced nitrogen inputs and escalated nitrogen losses might exacerbate nitrogen scarcity. As a result, the global forest C sink is projected to decline by 41% by the end of the century. The effects of warming on the global nitrogen budget and forest carbon sinks suggest a consistent and robust trend across multiple scenarios (Supplementary Fig. 2).

Total nitrogen input shows an overall decline of 8%, equivalent to 7 ± 2 Tg N yr^{-1} (from 92 ± 29 Tg N yr^{-1} to 85 ± 26 Tg N yr^{-1}) (Fig. 3). Spatial discrepancies in nitrogen inputs are mainly attributable to shifts in BNF and nitrogen deposition in global forests (Fig. 3). These changes show a global imbalance, with substantial decreases in lower latitudes and increases in higher latitudes in response to warming (Fig. 2a). The largest projected declines in nitrogen inputs are in tropical rainforests, particularly in the Amazon and Congo basins, South Asia, Southeast Asia, and northern Australia. One plausible explanation is that the
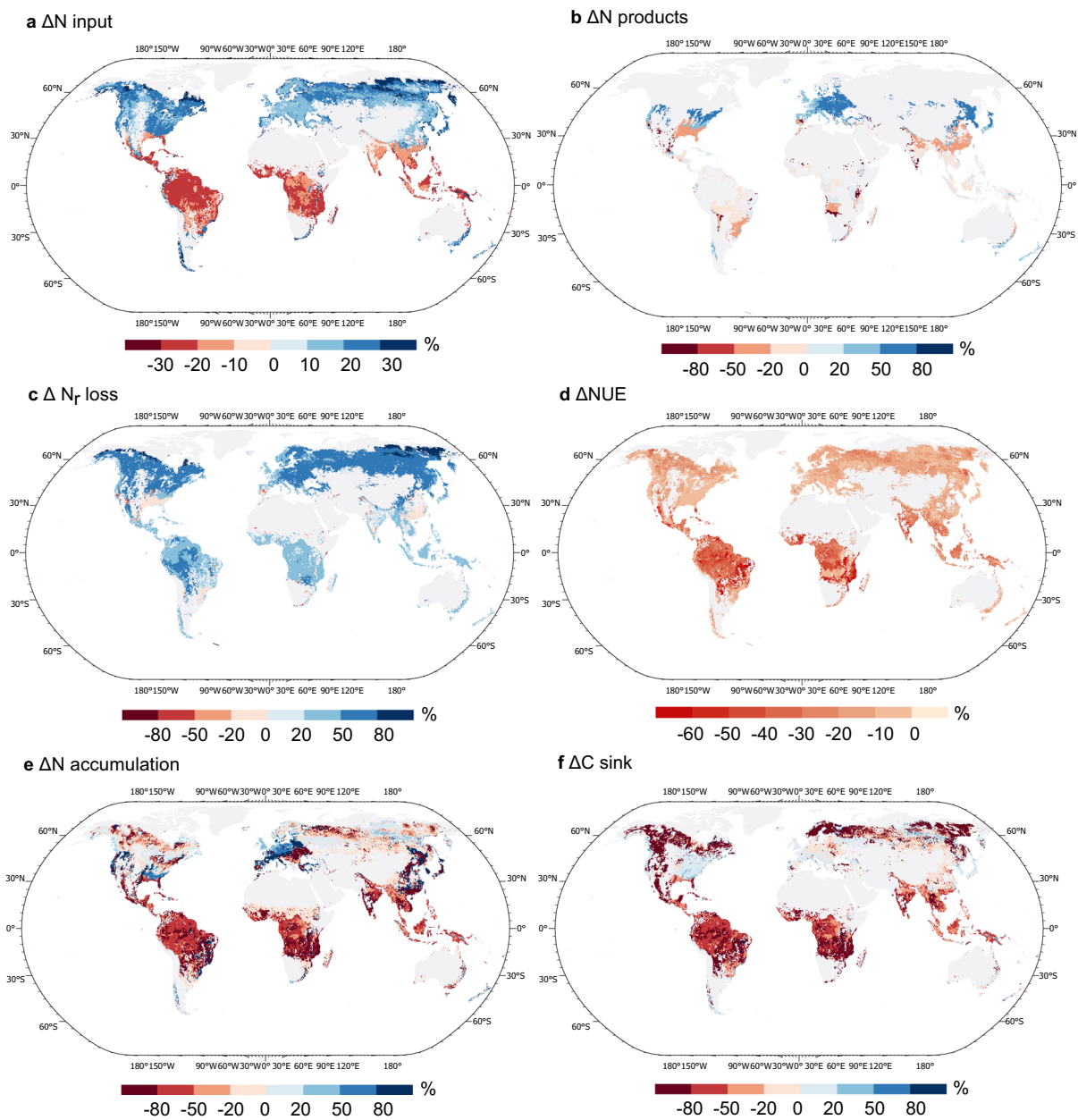
Fig. 2 | Spatial changes in nitrogen and carbon budgets of global forests in 2100 under SSP5-8.5 warming scenario. Warming-induced changes in (**a**) total nitrogen input (ΔN input), (**b**) nitrogen in forest products (ΔN products), (**c**) reactive nitrogen loss (ΔN$_r$ loss), (**d**) nitrogen use efficiency (ΔNUE), (**e**) nitrogen accumulation in living biomass and soil stock (ΔN accumulation), (**f**) carbon sink (ΔC sink). Values in the legends represent the average nitrogen budget within a pixel (0.5 by 0.5°). Source data are provided as a Source Data file.

rising temperatures in this high-emission scenario by the end of the century may exceed the optimal temperature for BNF[8], particularly in (sub)tropical forests at lower latitudes. This would result in reduced BNF rates (Supplementary Fig. 3a). Altitudinal factors are also critical in explaining these differences, with high-altitude areas typically showing a positive response to warming due to their cooler baseline temperatures. This response is pronounced in regions such as the Andes in South America, the highlands of eastern and southern Africa, and the highlands of Papua New Guinea in the South Pacific. Furthermore, projections indicate an upward trajectory of global nitrogen deposition (Supplementary Fig. 3b), possibly driven by increased atmospheric emissions of nitrogen gases under warming, thereby promoting a positive feedback mechanism for nitrogen inputs.

Nitrogen outputs from N products are projected to increase from 23 ± 7 Tg N yr⁻¹ to 27 ± 8 Tg N yr⁻¹, showing an asymmetric response to warming globally (Figs. 3 and 2b). This trend suggests an untapped potential for increased forest productivity in response to rising temperatures by 2100 across different biomes. The largest increases in N products are expected at mid- to high-latitude sites in the Northern Hemisphere, particularly in North America, Europe and East Asia. However, a decrease in N products is projected for certain tropical and subtropical forests in areas of South America, Africa, and South Asia. This is likely due to future temperatures exceeding the optimal range for vegetation photosynthesis under the warming scenario[21], leading to a drastic decrease in productivity, consistent with previous findings in tropical forests[34].
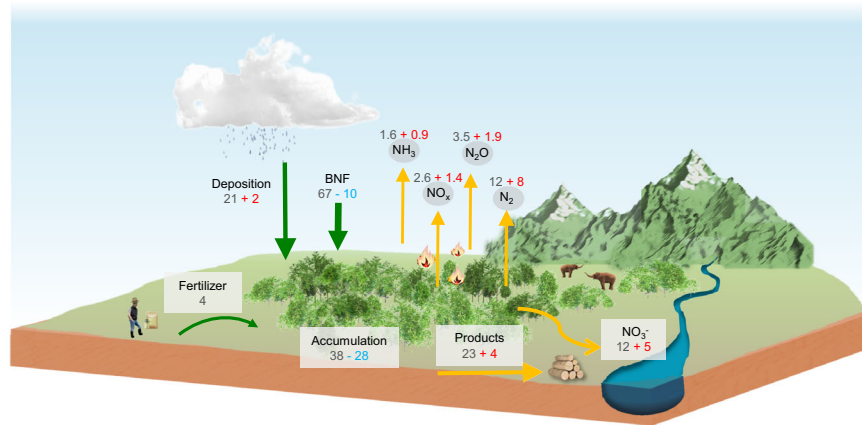
Fig. 3 | Nitrogen flows in global forests in 2100 under SSP5-8.5 warming scenario. Green and yellow arrows represent nitrogen input and output, respectively. Gray values illustrate nitrogen flows in the baseline. Red and blue values indicate increases and decreases of the nitrogen flows due to warming, respectively. The unit for these values is Tg N yr^{-1}. The decrease in total BNF is largely attributable to the rising temperatures by the end of the century under this high-emission scenario, which may exceed the optimal temperature for biological nitrogen fixation (BNF), particularly in tropical forests. Source data are provided as a Source Data file.

The possible escalating trend of N_r losses by 48%, equivalent to 9 ± 3 Tg N yr^{-1} (from 19 ± 6 Tg N yr^{-1} to 29 ± 8 Tg N yr^{-1}) (Fig. 3), is prevalent in most forests, with certain regions experiencing slight reductions (Fig. 2c). This trend is mainly attributed to various forms of gaseous N_r emissions (Supplementary Fig. 4), as well as nitrate leaching and runoff into aquatic systems (Supplementary Fig. 5). The largest increases in N_r losses are projected to occur primarily in the western and southeastern United States, northwestern South America, western Europe, central and western sub-Saharan Africa, East Asia, and Southeast Asia. Regions with reduced N_r losses are sporadically distributed in latitudes below 30 degrees north and south, likely as a result of heat stress-induced declines in nitrogen inputs and productivity. Thus, there's a discernible global downward trend in forest NUE due to widespread increases in N_r losses (Fig. 2d). The most drastic reductions will occur in tropical forests in areas such as Latin America, sub-Saharan Africa, South Asia, and Southeast Asia, followed by northern forests in North America and Eurasia.

Forest N accumulation tends to decrease globally by 75%, which is equivalent to 28 ± 9 Tg N yr^{-1} (from 38 ± 12 Tg N yr^{-1} to 10 ± 3 Tg N yr^{-1}) (Fig. 3). Decreases in N accumulation are expected in most regions, with the most pronounced decreases in the Amazon and Congo basins and in Southeast Asia (Fig. 2e). In contrast, small increases in N accumulation are expected in selected areas, including parts of North America and the northern Eurasian landmass. High elevation zones, such as mountain ranges and highlands, also show positive shifts in N accumulation. Correspondingly, the C sink capacity of global forests is projected to decrease by 0.45 ± 0.14 Pg C yr^{-1} (from 1.10 ± 0.34 Pg C yr^{-1} to 0.65 ± 0.20 Pg C yr^{-1}). The spatial dynamics of these changes are highly variable (Fig. 2f), with the most substantial reductions expected in the Amazon and Congo basins, while increases are projected primarily for North America. Other regions, including Europe, Asia, and Australia, show a high degree of spatial variability in carbon sink responses, with areas experiencing both declines and increases. This may be due to the trade-off between the dual effects of warming on carbon cycling: while increasing vegetation productivity, warming also increases carbon losses.

Impact assessment on forest assets

Based on projected changes in carbon and nitrogen cycles, we conducted a monetary assessment of the impact of warming as a single driver of climate change on global forest assets, taking into account ecosystem well-being, climate influence (including the effects of forest carbon sequestration and N_r on climate), and forest production (including the economic value of forest products and their production costs) (Fig. 4a). Overall, the impacts of warming on forests are expected to exacerbate the global development gap between the Global South and the Global North.

Warming is likely to pose a substantial threat to the economies of the Global South, particularly in tropical and arid regions. Most countries in the Global South will experience negative impacts from warming, mainly from ecosystem and climate damages, especially in sub-Saharan Africa (-US$ 6-17 billion), Latin America (except Brazil, -US$ 8-12 billion), other Asian countries (excluding China, -US$ 7–18 billion), and India (-US$ 4-14 billion)for 2100 (Fig. 4a). The negative impact on forest assets in the Global South remains a consistent trend across all scenarios, exacerbating pre-existing economic development challenges in the majority of countries in the Global South. In particular, regions such as the Amazon Basin, Congo Basin, and South and Southeast Asia are expected to experience substantial net damages under the SSP5-8.5 warming scenario during the 2040–2100 period (Fig. 5).

Conversely, net benefits are expected in higher latitudes under all future warming scenarios. Regions such as Europe (+US$ 83–124 billion), North America (+US$ 54–118 billion), the Former Soviet Union (+US$ 36–95 billion), and other Organization for Economic Cooperation and Development (OECD) countries (+US$ 15–19 billion) are projected to experience net benefits by the end of the 21st century (Fig. 4a). This is because in these regions, the effects of warming on forest production are expected to generate notable benefits that offset damages resulting from other aspects. Many of these regions are located in the Global North. Consequently, economies in the Global North, particularly in temperate and cold climates, are expected to experience more favorable impacts, thereby reinforcing their leading economic positions and further widening the global development gap[35].

The unique situations in Brazil and China should be highlighted. Both countries face significant reductions in total benefits under the higher emissions scenarios of SSP2-4.5 and SSP5-8.5 compared to SSP1-2.6, with the potential for these benefits to turn into net losses. Under the SSP1-2.6 warming scenario, Brazil and China are projected to have positive net benefits of US$38 billion and US$122 billion, respectively, in 2100 (Fig. 4a). Under the SSP5-8.5 warming scenario, Brazil is projected to have net damages of US$29 billion, while China is projected to have net benefits of US$9 billion in 2100. This is due to the vast territories of these countries, with some of their forests located within a latitudinal range of about 30° north to south. As global warming intensifies, the geographic extent of net damages from warming is projected to gradually shift from lower to higher latitudes (Fig. 5).
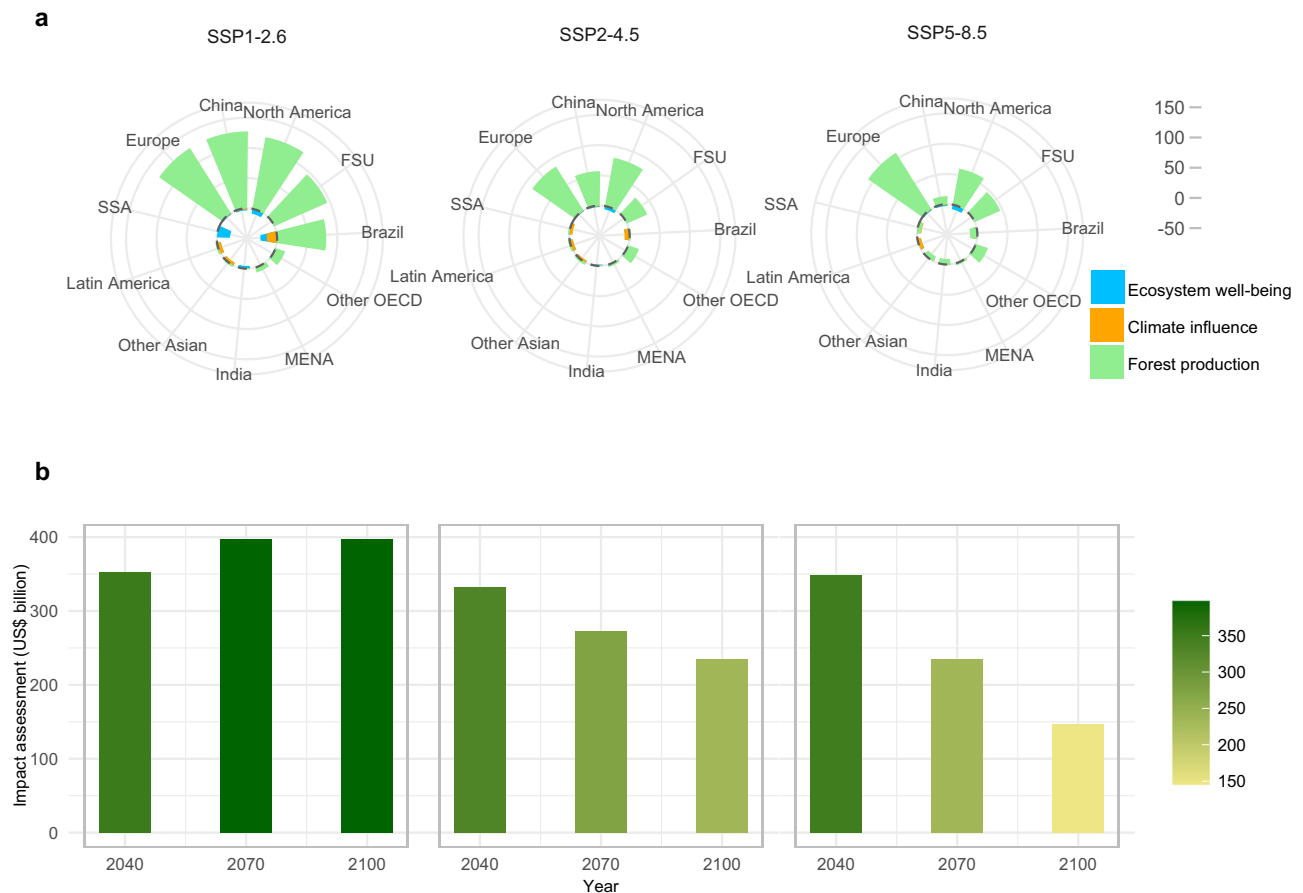
Fig. 4 | Impact assessment of warming on global forest assets. a Impact assessment by regions under multiple future scenarios (SSP1-2.6, SSP2–4.5, SSP5-8.5) for 2100. SSA, sub-Saharan Africa; FSU, Former Soviet Union; OECD, Organization for Economic Cooperation and development; MENA, Middle East and North Africa; Latin America, except Brazil. **b** Global impact assessment under future scenarios (SSP1-2.6, SSP2-4.5, SSP5-8.5) from 2040 to 2100. Values are in US$ billion. Source data are provided as a Source Data file.

Expanding global inequality over time

The impact of warming on global forest assets is expected to evolve over time under multiple scenarios (Fig. 4b). In addition, different socioeconomic pathways may influence the magnitude of global total benefits and even alter the direction of impacts in specific regions, as noted above for Brazil and China. In the SSP1-2.6 scenario, global total benefits increase over time, rising from US$352 billion in 2040 to US$397 billion in 2100. In the SSP2-4.5 and SSP5-8.5 warming scenarios, however, global benefits are projected to decline steadily over time, from US$332 billion and US$348 billion in 2040 to US$235 billion and US$146 billion in 2100, respectively. This is primarily due to the expected increase in global temperatures in both the SSP2-4.5 and SSP5-8.5 scenarios, which will cause some regions to experience temperatures above the optimal range for photosynthesis, reducing the benefits of forest production and even causing a shift from benefits to damages (Fig. 5 and Supplementary Fig. 6).

Under the SSP5-8.5 warming scenario, which represents high emissions in a fossil-fueled society, benefits decline sharply, reaching a minimum of US$146 billion by 2100 among all the scenarios (Fig. 4b). From the 0.5 by 0.5-degree map of the SSP5-8.5 impact assessment, many regions show a trend of shifting from net benefits to net damages starting in 2070, such as East Asia, Southeast Asia, parts of the eastern United States, and southeastern Latin America (Fig. 5). High-income countries (shown in gold) are mainly located in high-latitude regions and continue to benefit (Supplementary Fig. 7 and Fig. 5). In contrast, low-income and lower-middle-income regions near the equator (shown in dark and light purple, respectively) are likely to suffer varying degrees of damage under different scenarios. Upper-middle-income countries (in blue) face mixed impacts of both benefits and damages, depending on their latitude and climate zone, and their vulnerability to damages will increase as warming intensifies. For 2100, under the SSP5-8.5 warming scenario, high-income countries are projected to still accumulate US$179 billion in benefits, while low-income, lower-middle-income, and upper-middle-income countries will experience net losses totaling US$31 billion.

Future perspective

Our findings demonstrate that warming would drive widespread vegetation succession, coupled with increased nitrogen depletion, potentially undermining carbon sequestration capacity of global forests. Adopting a sustainable model of societal development can maximize the benefits to humanity from forest resources, while significantly advancing the threshold for warming benefits relative to a high-emissions society. In the SSP5-8.5 fossil-fueled society, the worst-case scenario is projected to unfold, with certain regions exceeding the optimal temperature for photosynthesis after 2070. As a result, the warming impact in these areas is expected to shift from positive to negative. While our current projections extend to 2100, it is important to recognize that if global temperatures continue to rise, more forests may exceed their optimal photosynthetic temperature in the new century. This could lead to declining productivity and more severe negative impacts. Some studies also suggest that productivity growth potential in the Northern Hemisphere may plateau after 2070[9],
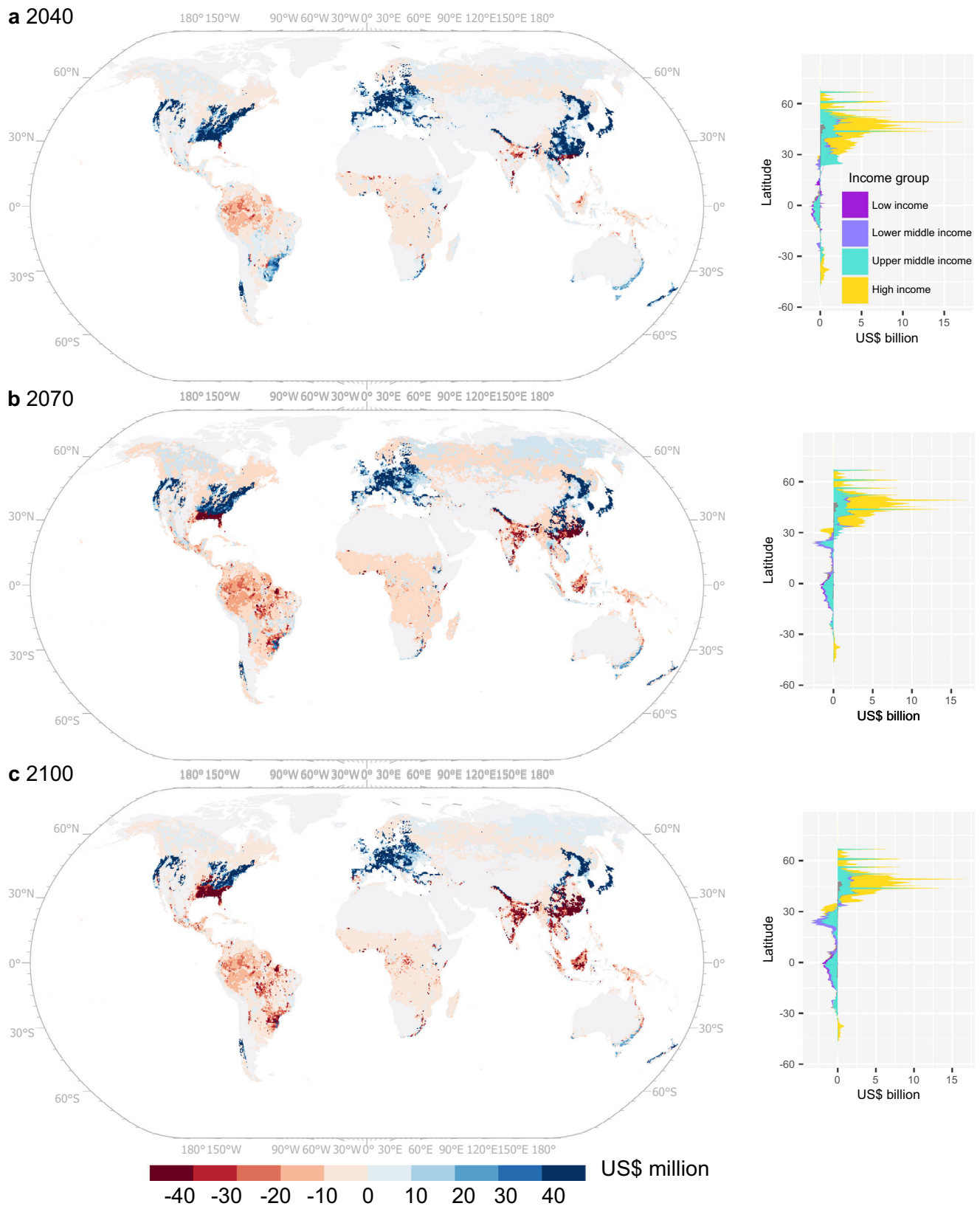
Fig. 5 | Global distribution patterns of the monetized warming impact on forests. Global variations in monetized values of warming impact on forests under SSP5-8.5 (left panel) and monetized values across latitudes by income groups (right panel) for 2040 (**a**), 2070 (**b**), and 2100 (**c**). Values depicting spatial changes are in US$ million for each 0.5 by 0.5-degree pixel. Source data are provided as a Source Data file.

implying a prolonged elevated risk under future warming. Additionally, warming-induced higher nitrogen losses in forests, leading to successive reductions in nitrogen accumulation, pose a dual threat to environmental quality and carbon sequestration capacity. The urgency of limiting global warming to within 1.5 or 2 °C can, therefore, not be overstated[36]. There is also an urgent need to improve long-term dynamic monitoring of forests in order to detect risks related to global warming in a timely manner[15].

Simultaneously, it is crucial to recognize that the impact of warming on forest assets displays notable spatial inequality. Regardless of the scenario, low-income countries in tropical and arid climates will face adverse effects, underscoring the need for early support and action to mitigate these impacts[37]. It is essential to develop climate-smart forest management strategies that facilitate forest adaptation to warming, focusing on succession, carbon sequestration, and nitrogen retention. This can be achieved primarily through proactive measures to minimize the adverse effects of warming, such as comprehensive conservation and restoration, optimizing tree species composition, cultivating adaptive species, and adjusting planting and harvesting schedules for plantations[38]. Some ecosystem-based adaptation projects have been implemented in the Global South, including the restoration of Himalayan forests in Nepal, and the planting of drought-tolerant tree seedlings in the drylands of Mauritania[39]. It is crucial to tailor solutions to the specific ecological and socio-economic contexts of different regions or sites, requiring a thorough assessment of the full range of ecosystem goods and services following the implementation of management measures. For instance, conserving biodiversity has the potential to help forests adapt to future climate-induced succession, with benefits for carbon and nitrogen cycling in forest ecosystems[40]. However, in some cases there may be inconsistent responses to these interventions, highlighting the need for careful, context-specific planning[41,42].

In addition, our study has limitations related to data sources and modeling techniques. Logistical challenges have resulted in relatively sparse warming experiment data for tropical forests in the Southern Hemisphere, limiting the availability of field data in countries of the Global South. We validated our model results with other tropical forest studies to ensure comparability and evaluated the uncertainty ranges using Monte Carlo simulations (Supplementary Discussion). However, more experiments and measurements in the Southern Hemisphere are needed to obtain first-hand data and to minimize potential biases in the modeling. It is also important to recognize that warming is only one of several drivers of climate change. Future research on the responses of carbon and nitrogen cycles to climate change should consider the interaction of warming with other factors, including drought and wildfire. Warming increases transpiration and drought in forests, thus water availability may mediate the nonlinear feedback of biogeochemical cycles to climate warming (e.g., vegetation growth[43] and productivity[44], carbon sink[10]). In addition, warming-induced higher aridity may amplify the risk of wildfires[45,46]. Some empirical studies have found evidence of increased tree mortality in Canadian boreal forests[47] and declined primary productivity across European northern forests[48] due to regional droughts and heatwaves. Recent satellite observations indicate that global vegetation greening is reaching near-record levels, while extreme events may be responsible for regional browning[49]. Currently, our study is limited to warming as the sole driver of climate change, except that the climate data have accounted for the interaction of temperature and precipitation. Therefore, a further understanding of the interplay between warming and other drivers is needed to obtain a realistic picture of the trade-offs under climate change and to formulate adaptation and mitigation strategies in forests[50]. In the worst case scenario, if declining productivity in northern forests becomes a reality in the future, we will not be able to count on the expected benefits from this region as a potential offset[51].

Methods

Global synthesis of warming experiments in forests

We have compiled data from warming experiments (Supplementary Table 1) and additional open data sources to construct a comprehensive global dataset of warming experiments in forest ecosystems. We consulted the Manipulation Experiments Synthesis Initiative (MESI) database[52] and performed a cross-search to identify eligible studies based on the following criteria (see Preferred Reporting Items for Systematic Reviews and Meta-Analyses, PRISMA flowchart as Supplementary Fig. 8): (1) warming experiments with control (ambient temperature) and treatment (elevated temperature) groups, including both field and incubation experiments; (2) measurements of variables associated with nitrogen and carbon cycles, such as BNF, N_2O, NO_3^-, nitrogen/carbon content, NPP, soil respiration, and etc.; (3) studies published in peer-reviewed journals and indexed in authoritative databases such as Web of Science, Google Scholar, and Scopus. The systematic literature search focused on, but was not restricted to, these key terms: {(elevated temperature/increasing temperature/warming) AND {(forest/tree/seedling/shrub) AND {(nitrogen fixation/BNF/nitrogen use efficiency/NUE/denitrification/ammonia/NH3/nitrous oxide/N2O/nitrate/mineralization/nitrification/nitrogen) OR (net primary productivity/NPP/soil organic carbon/SOC/soil respiration/Rs/carbon)}.

From textual descriptions, tables, and figures, we extracted information about study sites, experimental design, and variable specifications. We used WebPlotDigitizer 4.4 (https://apps.automeris.io/wpd/) for data extraction from figures. In addition, we collected supplementary climate information, soil data, and climatic zone classifications for specific study sites from external open data sources when relevant information was missing. Historical and future climate data were obtained from the WorldClim database (https://worldclim.org/data/index.html#). Soil data were sourced from the Global Land Data Assimilation System (GLDAS) (https://ldas.gsfc.nasa.gov/gldas/soils). Climate zones were determined based on the Köppen-Geiger climate classification[53].

We utilized multi-level meta-analyses organized into three tiers: (i) individual observations, (ii) climatic domain (such as boreal, temperate, (sub)tropical), and (iii) the global scale. An observation in the context of a forest warming experiment is a record of a variable of interest, including measurements from both the control and warming groups at a given time or for a given period of time.

To calculate the response ratio (effect size) for each individual observation, we utilized the natural logarithm of the response ratio ($\ln R$) formula[54], as shown below:

$$\ln R = \ln \frac{x_{eT}}{x_{aT}} \tag{1}$$

where x_{eT} and x_{aT} represent the means of parameters at elevated temperature and ambient temperature, respectively.

The weight assigned to each individual observation was determined according to the number of experimental replications, and the variance was calculated as the reciprocal of the weight using the following equations:

$$\text{Weight} = \frac{n_{eT} \times n_{aT}}{n_{eT} + n_{aT}} \tag{2}$$

$$\text{Variance} = \frac{1}{\text{Weight}} \tag{3}$$

where n_{eT} and n_{aT} denote the number of replications at elevated temperature and ambient temperature levels, respectively.

We then calculated the weighted mean response ratios (RR) with 95% confidence intervals (CI) for tier ii and tier iii using a mixed effects

model[55], with 'site' included as a random factor to account for non-independence at the site level. The 95% CI defines the lower and upper bounds of the overall mean. An RR is considered statistically significant ($P < 0.05$) if its 95% CI excludes zero. The meta-analysis was performed using the *metafor* package on the R platform (version 4.1.3)[56]. The results are presented as percentage changes in response ratios for clarity, using the following equation:

$$RR\% = (e^{RR} - 1) \times 100\% \tag{4}$$

Carbon and nitrogen budgets in global forests

In this study, we estimated the global forest carbon and nitrogen budgets using DLEM[30,31] and CHANS models[32,33] (Supplementary Fig. 1). These estimates were generated at a spatial resolution of 0.5 degrees by 0.5 degrees. We adopted a multi-model simulation approach to establish robust global forest carbon and nitrogen budgets, aiming to minimize uncertainties. The gridded data generated by the DLEM model were systematically integrated into the CHANS model. This integration involved a comprehensive comparison and calibration process with the nationally-scaled data embedded within the CHANS model.

The DLEM model is a dynamic global vegetation model specifically designed to simulate daily variations in carbon, water, and nitrogen dynamics. It incorporates a wide range of factors, such as atmospheric chemistry, climate patterns, land-use changes, and disturbances[31].

To calculate plant net primary productivity (NPP$_i$) at the grid level i, the following equations were applied:

$$NPP_i = GPP_{sun,i} + GPP_{shade,i} - G_{r,i} - M_{r,i} \tag{5}$$

$$GPP_{sun,i} = 12.01 \times 10^{-6} \times A_{sun,i} \times LAI_{sun,i} \times dayl_i \times 3600 \tag{6}$$

$$GPP_{shade,i} = 12.01 \times 10^{-6} \times A_{shade,i} \times LAI_{shade,i} \times dayl_i \times 3600 \tag{7}$$

$$G_{r,i} = 0.125 \times (GPP_{sun,i} + GPP_{shade,i}) \tag{8}$$

where $GPP_{sun,i}$ and $GPP_{shade,i}$ represent the gross primary productivity for the sunlit and shaded canopy, respectively; $G_{r,i}$ represents the growth respiration of plants; $M_{r,i}$ denotes the maintenance respiration; $A_{sun,i}$ and $A_{shade,i}$ are the leaf-level assimilation rates of the sunlit and shaded canopy, respectively, calculated using the model proposed by Farquhar et al[57].; $LAI_{sun,i}$ and $LAI_{shade,i}$ are the projected leaf area indices for the sunlit and shaded canopy, respectively; $dayl_i$ denotes the duration of daylight in hours within a day.

The LAI_{sun} is calculated using the following equation[58]:

$$LAI_{sun} = 2\cos\theta_{ave}(1 - e^{-0.5\Omega LAI/\cos\theta_{ave}}) \tag{9}$$

where Ω is a plant functional type (PFT) specific parameter to represent foliage clumping effect, LAI is the total leaf area index, θ_{ave} is daily average zenith angle.

The LAI_{shade} is calculated using the following equation:

$$LAI_{shade} = LAI - LAI_{sun} \tag{10}$$

Maintenance respiration (M_r) of plants is influenced by surface air temperature and the carbon content present in various plant components, including leaves, sapwood, fine roots, and coarse roots. The calculation of M_r involves the aggregation of carbon pools across all plant parts as follows:

$$M_{r,i} = \sum(\min(Rsep_{coef} \times f(T), r_{max}) \times CV_m) \tag{11}$$

where $Rsep_{coef}$ represents a respiration coefficient specific to each plant functional type; The temperature factor, denoted as $f(T)$, is calculated as a function of the daily average air temperature; r_{max} represents the maximum respiration rate for different carbon pools; CV_m corresponds to the carbon content of vegetation pool m.

The calculation of r_{max} is determined by the following equation:

$$r_{max} = \left(\sum_{i=1}^{5} C_i - C_{seed}\right) / \sum_{i=1}^{5} C_i \tag{12}$$

where C_{seed} is PFT specific seed carbon. In order to simulate germination, vegetation carbon is assumed no less than C_{seed}.

A Q_{10} function is adopted to calculate temperature factor, $f(T)$, as follows:

$$f(T) = Q_{10}^{\frac{T-25}{10}} \tag{13}$$

For aboveground biomass, such as leaf, sapwood, and reproduction pools, T is air temperature; for belowground pools such as coarse root and fine root, T is the average soil temperature of the upper 50 cm.

The calculation of the net biome productivity at time t (NBP$_t$) is determined by the following equation:

$$NBP_t = (CV_t + CS_t + CL_t + CP_t) - (CV_{t-1} + CS_{t-1} + CL_{t-1} + CP_{t-1}) \tag{14}$$

where CV_t, CS_t, CL_t, and CP_t denote the carbon content of the vegetation pool, soil pool, litter pool, and product pool at time t, respectively; CV_{t-1}, CS_{t-1}, CL_{t-1}, and CP_{t-1} represent the carbon content of these pools at time $t-1$, respectively.

The CHANS model is a nitrogen cycle model designed to simulate nitrogen flows within various interconnected subsystems at the interface of the natural and human environment[32,33].

The calculation of the forest nitrogen budget is performed at the grid i level based on the mass balance principle using the following equations:

$$\sum_1^k N_{input,i} = \sum_1^k N_{BNF,i} + \sum_1^k N_{deposition,i} + \sum_1^k N_{fertilizer,i} \tag{15}$$

$$\sum_1^k N_{input,i} = \sum_1^k N_{r,i} + \sum_1^k N_{2,i} + \sum_1^k N_{products,i} + \sum_1^k N_{accumulation,i} \tag{16}$$

$$\sum_1^k N_{r,i} = \sum_1^k NH_{3,i} + \sum_1^k N_2O_{,i} + \sum_1^k NOx_{,i} + \sum_1^k NO_{3,i}^- \tag{17}$$

$$NUE_i = \frac{N_{products,i} + N_{accumulation,i}}{N_{input,i}} \tag{18}$$

where $N_{input,i}$ represents the total N input, consisting of BNF ($N_{BNF,i}$), nitrogen deposition ($N_{deposition,i}$), and synthetic fertilizer ($N_{fertilizer,i}$). Here, nitrogen fertilizer as a minor anthropogenic input is restricted to some managed forests, especially plantations and nitrogen-poor forests[59–61] (Supplementary Fig. 9). $N_{input,i}$ also equals to the sum of total nitrogen output, including reactive nitrogen ($N_{r,i}$), N_2 emissions ($N_{2,i}$), the quantity of nitrogen in both timber and non-timber forest products ($N_{products,i}$), and the N increment in living biomass, litterfall, and soil stock ($N_{accumulation,i}$); $N_{r,i}$ includes gaseous NH_3, N_2O, and NO_x emissions, as well as nitrate lossing to water bodies (NO_3^-); NUE_i denotes nitrogen use efficiency at grid i.

The loss factor ($F_{loss,i}$) are defined as:

$$F_{loss,i} = \frac{N_{com,i}}{N_{surplus,i}} \tag{19}$$

where $N_{com,i}$ could be any component of nitrogen loss; $N_{surplus,i}$ is the sum of reactive nitrogen and non-reactive N_2.

Scenario design and model simulation

In this study, we formulated two sets of scenarios: (i) Baseline scenarios: These scenarios assume no climate change and encompass SSP1 ('Sustainable society'), SSP2 ('Middle road'), and SSP5 ('Fossil-fueled society'). (ii) Warming scenarios: These scenarios focus solely on the impact of warming as the primary driver of climate change and include SSP1-2.6, SSP2-4.5, and SSP5-8.5, corresponding to 'Sustainable society', 'Middle road', and 'Fossil-fueled society', respectively. Future temperature projections under different socioeconomic pathways are Coupled Model Intercomparison Project Phase 6 (CMIP6) downscaled future climate projections from WorldClim database (https://worldclim.org/data/index.html#). Additionally, future forest areas were derived from the Global Change Analysis Model for future land use projections[62].

Subsequently, we conducted model simulation under various scenarios. The effects of warming on forest carbon and nitrogen variables were integrated into the forest products based on climatic domain and temperature optima of vegetation productivity under future warming scenario within grid i using the following equations:

$$N_{products,i}^{eT} = N_{products,i}^{base} \times (1 + RR\%_{NPP,i}) \times (1 + RR\%_{stem[N],i}) \tag{20}$$

where $N_{products,i}^{eT}$ and $N_{products,i}^{base}$ represent the nitrogen in the forest products under the warming scenario and baseline scenario, respectively; $RR\%_{NPP,i}$ and $RR\%_{stem[N],i}$ denote the response ratios of NPP and stem nitrogen content to warming. Here net photosynthesis is used as a proxy for NPP in the meta-analysis. When the temperature optima of the productivity are exceeded, the negative response is dominant in the forest or the positive response is dominant (Supplementary Fig. 10). The temperature optima of vegetation productivity for different climatic domains were obtained from a previous global synthesis[21].

The total nitrogen input under warming (N_{input}^{eT}) is obtained by summing up all the nitrogen input components within grid i as follows:

$$N_{input,i}^{eT} = N_{BNF,i}^{eT} + N_{deposition,i}^{eT} + N_{fertilizer,i}^{eT} \tag{21}$$

where the BNF under the warming scenario ($N_{BNF,i}^{eT}$) is attained by integrating the effects of warming and the optimal temperature[8] on the base BNF rates; nitrogen deposition under the warming scenario ($N_{deposition,i}^{eT}$) is obtained by integrating the effects of warming on baseline nitrogen deposition as a function of summed NH_3 and NO_x emissions; fertilizer application is assumed to maintain a uniform rate per unit of forest area fertilized.

As for the calculation of nitrogen loss, the effects of warming were incorporated to the component of nitrogen loss within grid i as follows:

$$N_{loss,i}^{eT} = N_{loss,i}^{base} \times (1 + RR\%_{Ncom,i}) \tag{22}$$

where $N_{loss,i}^{eT}$ and $N_{loss,i}^{base}$ represent the nitrogen loss under the warming and baseline scenarios, respectively; $RR\%_{Ncom,i}$ denotes the response ratio of any nitrogen loss component to warming. Since NH_3 and NO_x emissions from forests are minimal and metadata are insufficient, we use terrestrial mean response ratios as proxies.

The biome C: N ratio (CN_{bio}) is calculated within grid i using the following equation:

$$CN_{bio,i} = \frac{NBP_i}{N_{products,i} + N_{accumulation,i}} \tag{23}$$

It is assumed that CN_{bio} under warming remains similar to that in baseline, according to the results of the meta-analysis. Here, $N_{products,i}$ and $N_{accumulation,i}$ are calibrated to account for the effects of warming in the warming scenarios. Consequently, NBP is calculated under the warming scenarios using the formula mentioned above.

Impact assessment

The economic impact analysis of warming (I_{eT}) as the sole driver of climate change is carried out at the grid level within global forests. This analysis takes into account the potential effects on various aspects, including ecosystem (I_{eco}), climate change ($I_{climate}$), and forest production (I_{pro}) within grid i, as outlined below:

$$I_{eT,i} = I_{eco,i} + I_{climate,i} + I_{pro,i} \tag{24}$$

The impact on the ecosystem is measured by calculating the changes in damage costs resulting from N_r effects within grid i, as expressed in the following equation[63,64]:

$$I_{eco,i} = \Delta N_{r,i} \times d_{eco,EU} \times \frac{WTP_j}{WTP_{EU}} \times \frac{PPP_j}{PPP_{EU}} \tag{25}$$

where $\Delta N_{r,i}$ represents the change in N_r under warming scenario relative to the baseline, encompassing NH_3, N_2O, NO_x, and NO_3^- losses at grid i; $d_{eco,EU}$ represents for the estimated ecosystem damage cost of N_r emission in the European Union (EU) based on the European N Assessment; WTP_j and WTP_{EU} denote the values of the willingness to pay for ecosystem service in the country/ area j and the EU, respectively; PPP_j and PPP_{EU} denote the purchasing power parity of the country/ area j and the EU. To account for data limitations, we extend the ecosystem damage cost of N_r emissions in the EU to other countries by applying adjustments for comparable ecosystem benefits worldwide using willingness to pay and purchasing power parity adjustments.

The assessment of climate impact is conducted by taking into account the influence of carbon sequestration and N_r losses on climate change within grid i, as described below[65]:

$$I_{climate,i} = \Delta C_i \times p_{C,i} + \Delta N_{r,i} \times d_{climate,i} \tag{26}$$

where the change in C sequestration under warming is estimated by multiplying change of carbon sequestration (ΔC_i) and the carbon price ($p_{C,i}$); we use the national carbon prices for calculation[66], and the missing values for some countries are supplemented with means of the income groups; the influence of N_r losses on climate change is estimated by multiplying change of N_r losses ($\Delta N_{r,i}$) and climate damage cost of N_r ($d_{climate,i}$). The effects of N_r on climate change can be positive or negative, i.e., N_2O contributes to climate warming as a potent greenhouse gas, while NO_x and NH_3 exert climate cooling give that they are precursors of aerosol reflecting long-wave solar radiation.

The monetary evaluation of forest production is performed by subtracting the production costs from the income generated by forest products. Production costs here primarily refer to fertilizers, while other costs such as infrastructure (i.e., road construction) and logging operations are not considered in this study. The equation used is as follows:

$$I_{pro,i} = \Delta N_{pro,i} \times p_{pro,i} - \Delta N_{fertilizer,i} \times p_{fertilizer,i} \tag{27}$$

where $\Delta N_{\mathrm{pro},i}$ denotes the changes in forest products under warming; the price of forest products ($p_{\mathrm{pro},i}$) is estimated by dividing the value of forest products traded by the quantity based on the FAO database (https://www.fao.org/faostat/en/#data/FAO); $\Delta N_{\mathrm{fertilizer},i}$ denotes the changes in N fertilizer under warming; the N fertilizer price ($p_{\mathrm{fertilizer},i}$) is estimated by dividing the value of fertilizers traded by the quantity based on the UN Comtrade Database (https://comtrade.un.org/). For countries with missing price data, we substitute the global average value.

Uncertainty analysis

To comprehensively assess model output uncertainties, we conducted an uncertainty analysis using Monte Carlo simulations with the CHANS model. We performed 1000 iterations to generate projection ensembles and calculate both the mean and variability of carbon and nitrogen budgets. Coefficients of variation (CV) were used to gauge the relative levels of uncertainty in carbon and nitrogen budgets data and the effects of warming on carbon and nitrogen dynamic (Supplementary Table 2).

Reporting summary

Further information on research design is available in the Nature Portfolio Reporting Summary linked to this article.

Data availability

All data supporting the findings of this study are openly available, and their sources are detailed in the Methods and Supplementary Information. The global dataset of forest warming experiments generated in this study are available in Figshare at https://doi.org/10.6084/m9.figshare.26124748. The climate data are available in the WorldClim database (https://worldclim.org/data/index.html#). The soil data are available in the Global Land Data Assimilation System (GLDAS, https://ldas.gsfc.nasa.gov/gldas/soils). The forest products data are available in the FAO database (https://www.fao.org/faostat/en/#data/FAO). The fertilizer price data are available in the UN Comtrade Database (https://comtrade.un.org/). Source data are provided with this paper.

Code availability

The codes used in the study are available in Figshare at https://doi.org/10.6084/m9.figshare.26124748.

References

1. FAO. *Global Forest Resources Assessment 2020: Main report.* Rome (2020).
2. Pan, Y. et al. A large and persistent carbon sink in the world's forests. *Science* **333**, 988–993 (2011).
3. Bonan, G. B. Forests and climate change: forcings, feedbacks, and the climate benefits of forests. *Science* **320**, 1444–1449 (2008).
4. DESA. *The Global Forest Goals Report 2021* (UN Department of Economic and Social Affairs (DESA), 2021).
5. Anderegg, W. R. L. et al. A climate risk analysis of Earth's forests in the 21st century. *Science* **377**, 1099–1103 (2022).
6. Gruber, N. & Galloway, J. N. An Earth-system perspective of the global nitrogen cycle. *Nature* **451**, 293–296 (2008).
7. Chen, W. et al. Evidence for widespread thermal optimality of ecosystem respiration. *Nat. Ecol. Evol.* **7**, 1379–1387 (2023).
8. Houlton, B. Z., Wang, Y. P., Vitousek, P. M. & Field, C. B. A unifying framework for dinitrogen fixation in the terrestrial biosphere. *Nature* **454**, 327–330 (2008).
9. Zhang, Y. et al. Future reversal of warming-enhanced vegetation productivity in the Northern Hemisphere. *Nat. Clim. Change* **12**, 581–586 (2022).
10. Quan, Q. et al. Water scaling of ecosystem carbon cycle feedback to climate warming. *Sci. Adv.* **5**, 1–8 (2019).
11. Yu, H. et al. Universal temperature sensitivity of denitrification nitrogen losses in forest soils. *Nat. Clim. Change* **13**, 726–734 (2023).
12. Reich, P. B. et al. Geographic range predicts photosynthetic and growth response to warming in co-occurring tree species. *Nat. Clim. Change* **5**, 148–152 (2015).
13. Pascual, U. et al. Diverse values of nature for sustainability. *Nature* **620**, 813–823 (2023).
14. Yin, J., Slater, L. J., Liu, P., Liu, D. & Cheng, J. Socio-economic inequality exacerbated by climate change. *Innov. Geosci.* **2**, 100078 (2024).
15. De Marco, A. et al. Strategic roadmap to assess forest vulnerability under air pollution and climate change. *Glob. Change Biol.* **28**, 5062–5085 (2022).
16. Zhang, J., Liu, C. & Xu, J. Earth Critical Zone: a comprehensive exploration of the Earth's surface processes. *Earth Crit. Zone* **1**, 100001 (2024).
17. Comstedt, D. et al. Effects of elevated atmospheric carbon dioxide and temperature on soil respiration in a boreal forest using $\delta^{13}C$ as a labeling tool. *Ecosystems* **9**, 1266–1277 (2006).
18. Lükewille, A. & Wright, R. F. Experimentally increased soil temperature causes release of nitrogen at a boreal forest catchment in southern Norway. *Glob. Change Biol.* **3**, 13–21 (1997).
19. Cusack, D. F., Torn, M. S., McDowell, W. H. & Silver, W. L. The response of heterotrophic activity and carbon cycling to nitrogen additions and warming in two tropical soils. *Glob. Change Biol.* **18**, 400–400 (2010).
20. Emmett, B. A. et al. The response of soil processes to climate change: Results from manipulation studies of shrublands across an environmental gradient. *Ecosystems* **7**, 625–637 (2004).
21. Huang, M. et al. Air temperature optima of vegetation productivity across global biomes. *Nat. Ecol. Evol.* **3**, 772–779 (2019).
22. Huang, G., Rymer, P. D., Duan, H., Smith, R. A. & Tissue, D. T. Elevated temperature is more effective than elevated [CO_2] in exposing genotypic variation in Telopea speciosissima growth plasticity: Implications for woody plant populations under climate change. *Glob. Change Biol.* **21**, 3800–3813 (2015).
23. Noh, N. J. et al. Responses of soil, heterotrophic, and autotrophic respiration to experimental open-field soil warming in a cool-temperate deciduous forest. *Ecosystems* **19**, 504–520 (2016).
24. Sun, Y. et al. A global meta-analysis on the responses of C and N concentrations to warming in terrestrial ecosystems. *Catena* **208**, 105762 (2022).
25. Schindlbacher, A., Schnecker, J., Takriti, M., Borken, W. & Wanek, W. Microbial physiology and soil CO_2 efflux after 9 years of soil warming in a temperate forest - no indications for thermal adaptations. *Glob. Change Biol.* **21**, 4265–4277 (2015).
26. Tian, Y. et al. Long-term warming of a forest soil reduces microbial biomass and its carbon and nitrogen use efficiencies. *Soil Biol. Biochem.* **184**, 109109 (2023).
27. Walker, T. W. N. et al. Microbial temperature sensitivity and biomass change explain soil carbon loss with warming. *Nat. Clim. Change* **8**, 885–889 (2018).
28. Fowler, D. et al. The global nitrogen cycle in the twenty-first century. *Philos. Trans. R. Soc. B Biol. Sci.* **368**, 20130164 (2013).
29. Saad, O. A. L. O. & Conrad, R. Temperature dependence of nitrification, denitrification, and turnover of nitric oxide in different soils. *Biol. Fertil. Soils* **15**, 21–27 (1993).
30. You, Y. et al. Incorporating dynamic crop growth processes and management practices into a terrestrial biosphere model for simulating crop production in the United States: toward a unified modeling framework. *Agric. Meteorol.* **325**, 109144 (2022).
31. Tian, H. et al. Model estimates of net primary productivity, evapotranspiration, and water use efficiency in the terrestrial ecosystems of the southern United States during 1895-2007. *Ecol. Manag.* **259**, 1311–1327 (2010).
32. Gu, B. et al. Cost-effective mitigation of nitrogen pollution from global croplands. *Nature* **613**, 77–84 (2023).

33. Gu, B. et al. Toward a generic analytical framework for sustainable nitrogen management: application for China. *Environ. Sci. Technol.* **53**, 1109–1118 (2019).

34. Nölte, A., Yousefpour, R., Cifuentes-Jara, M. & Hanewinkel, M. Sharp decline in future productivity of tropical reforestation above 29 °C mean annual temperature. *Sci. Adv.* **9**, eadg9175 (2023).

35. Esperon-Rodriguez, M. et al. Climate change increases global risk to urban forests. *Nat. Clim. Change* **12**, 950–955 (2022).

36. McKay, D. I. A. et al. Exceeding 1.5 °C global warming could trigger multiple climate tipping points. *Science* **377**, eabn7950 (2022).

37. Roe, S. et al. Contribution of the land sector to a 1.5 °C world. *Nat. Clim. Change* **9**, 817–828 (2019).

38. Triviño, M. et al. Future supply of boreal forest ecosystem services is driven by management rather than by climate change. *Glob. Change Biol.* **29**, 1484–1500 (2023).

39. Mills, A. J. et al. Ecosystem-based adaptation to climate change: Lessons learned from a pioneering project spanning Mauritania, Nepal, the Seychelles, and China. *Plants People Planet* **2**, 587–597 (2020).

40. Hua, F. et al. The biodiversity and ecosystem service contributions and trade-offs of forest restoration approaches. *Science* **376**, 839–844 (2022).

41. D'Orangeville, L. et al. Beneficial effects of climate warming on boreal tree growth may be transitory. *Nat. Commun.* **9**, 1–10 (2018).

42. Grossiord, C. Having the right neighbors: how tree species diversity modulates drought impacts on forests. *New Phytol.* **228**, 42–49 (2020).

43. Jochner, M., Bugmann, H., Nötzli, M. & Bigler, C. Tree growth responses to changing temperatures across space and time: a fine-scale analysis at the treeline in the Swiss Alps. *Trees - Struct. Funct.* **32**, 645–660 (2018).

44. Li, X. et al. Global variations in critical drought thresholds that impact vegetation. *Natl Sci. Rev.* **10**, nwad049 (2023).

45. Brown, P. T. et al. Climate warming increases extreme daily wildfire growth risk in California. *Nature* **621**, 760–766 (2023).

46. Liang, L., Liang, S. & Zeng, Z. Extreme climate sparks record boreal wildfires and carbon surge in 2023. *Innovation* **5**, 100631 (2024).

47. Peng, C. et al. A drought-induced pervasive increase in tree mortality across Canada's boreal forests. *Nat. Clim. Change* **1**, 467–471 (2011).

48. Ciais, P. et al. Europe-wide reduction in primary productivity caused by the heat and drought in 2003. *Nature* **437**, 529–533 (2005).

49. Li, X. et al. Vegetation greenness in 2023. *Nat. Rev. Earth Environ.* **5**, 241–243 (2024).

50. Lassaletta, L. et al. Nitrogen dynamics in cropping systems under Mediterranean climate: a systemic analysis. *Environ. Res. Lett.* **16**, 073002 (2021).

51. Wang, J., Taylor, A. R. & D'Orangeville, L. Warming-induced tree growth may help offset increasing disturbance across the Canadian boreal forest. *Proc. Natl Acad. Sci. USA* **120**, 2017 (2023).

52. Van Sundert, K. et al. When things get MESI: The Manipulation Experiments Synthesis Initiative—A coordinated effort to synthesize terrestrial global change experiments. *Glob. Change Biol.* **29**, 1922–1938 (2023).

53. Beck, H. E. et al. Present and future köppen-geiger climate classification maps at 1-km resolution. *Sci. Data* **5**, 180214 (2018).

54. Hedges, L. V., Gurevitch, J. & Curtis, P. S. The meta-analysis of response ratios in experimental ecology. *Ecology* **80**, 1150 (1999).

55. Terrer, C., Vicca, S., Hungate, B. A., Phillips, R. P. & Prentice, I. C. Mycorrhizal association as a primary control of the CO_2 fertilization effect. *Science* **353**, 72–74 (2016).

56. Viechtbauer, W. Conducting meta-analyses in R with the metafor. *J. Stat. Softw.* **36**, 1–48 (2010).

57. Farquhar, G. D., von Caemmerer, S. & Berry, J. A. A biochemical model of photosynthetic CO_2 assimilation in leaves of C_3 species. *Planta* **149**, 78–90 (1980).

58. Norman, J. *Biometeorology in Integrated Pest Management*. Vol. 65 (Academic Press, 1982).

59. Smethurst, P. J. Forest fertilization: trends in knowledge and practice compared to agriculture. *Plant Soil* **335**, 83–100 (2010).

60. Bergh, J. & Hedwall, P. O. Fertilization in boreal and temperate forests and the potential for biomass production. *For. BioEnergy Prod.* **9781461483**, 95–109 (2013).

61. Pukkala, T. Optimal nitrogen fertilization of boreal conifer forest. *For. Ecosyst.* **4**, 2–11 (2017).

62. Chen, M. et al. Global land use for 2015–2100 at 0.05° resolution under diverse socioeconomic and climate scenarios. *Sci. Data* **7**, 1–11 (2020).

63. Kristal, S. L., Randall-Kristal, K. A. & Thompson, B. M. The society for academic emergency medicine's 2004-2005 emergency medicine faculty salary and benefit survey. *Acad. Emerg. Med.* **13**, 548–558 (2006).

64. Sobota, D. J., Compton, J. E., McCrackin, M. L. & Singh, S. Cost of reactive nitrogen release from human activities to the environment in the United States. *Environ. Res. Lett.* **10**, 025006 (2015).

65. Zhang, X. et al. Societal benefits of halving agricultural ammonia emissions in China far exceed the abatement costs. *Nat. Commun.* **11**, 1–10 (2020).

66. Dolphin, G. & Xiahou, Q. World carbon pricing database: sources and methods. *Sci. Data* **9**, 1–7 (2022).

Acknowledgements

Author contributions

B.G. and J.C. designed the study. J.C. analyzed the data and wrote the first draft of the paper. O.D. provided support for CHANS model. M.Z. provided support for meta-data collection and validation. X.Z. provided support for impact assessment. Z.B., N.P., and H.T. provided modeling support for DLEM. J.X. contributed to the discussion of the study. All authors contributed to the discussion and revision of the paper.

Competing interests

The authors declare no competing interests.

Additional information

Supplementary information The online version contains supplementary material available at https://doi.org/10.1038/s41467-024-53518-5.

Correspondence and requests for materials should be addressed to Baojing Gu.

Peer review information *Nature Communications* thanks Jian Yang who co-reviewed with Jianjian Kongand the other, anonymous, reviewers for their contribution to the peer review of this work. A peer review file is available.

Reprints and permissions information is available at http://www.nature.com/reprints

Publisher's note Springer Nature remains neutral with regard to jurisdictional claims in published maps and institutional affiliations.